Supporting Information

Dynamic Proton Coupled Electron Transfer Quenching as Sensing Modality in Fluorescent Probes

Rasmus K. Jakobsen, Stine G. Stenspil, Junsheng Chen, and Bo W. Laursen*

Nano-Science Center & Department of Chemistry, University of Copenhagen, Universitetsparken 5, 2100 Copenhagen, Denmark

*E-mail: bwl@chem.ku.dk

Table of contents:

§1. Experimental details

Fluorophores:

4-(4-hydroxyphenyl)-4,8-diaza-11-oxatriangulenium hexafluorophosphate (phenol-DAOTA) and 4-(4-methoxyphenyl)-8-methyl-4,8-diaza-12-oxatriangulenium hexafluorophosphate (anisole-DAOTA) were synthesized as described previously.[1]

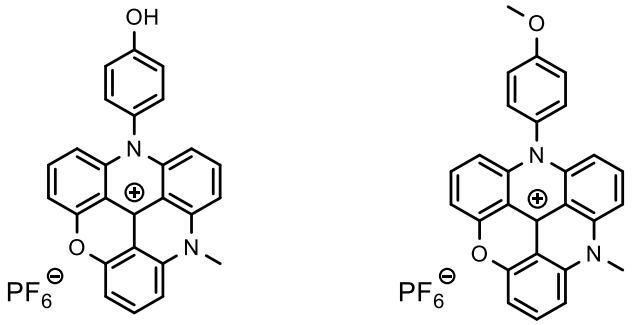

phenol-DAOTA anisole-DAOTA

Scheme 1. The probe phenol-DAOTA (left) and reference dye, anisole-DAOTA (right).

Materials and solvents:

All chemicals and solvents were purchased from Sigma-Aldrich, Riedel-de Haën, Merck, or VWR and used as received. Dimethyl sulfoxide (DMSO) and acetonitrile (MeCN) were of HPLC grade. Chemicals and solvents: Acetic acid and sodium acetate, L-valine, L-glutamic acid monosodium salt monohydrate, ethanolamine, sodium dihydrogen phosphate and disodium hydrogen phosphate, sodium chloride, formic acid, Glucose-6-phosphate, deuterium oxide, sodium deuteroxide, and deuterium chloride.

3,3-Diethyloxadicarbocyanine iodide (DODC) was purchased from abcr.

Water was purified using a MilliQ system (18.2 MΩcm, TOC<5 ppm).

Stock solutions of dyes were prepared in DMSO (10^{-4} M) and stored at ~5 °C in the dark when not in use to avoid degradation by exposure to light and heat.

Buffers:

All buffers were prepared following standard procedures with MilliQ water as the solvent.

Buffers include: Acetic acid, Valine, Glutamic acid, Ethanolamine, Phosphate buffer, Formic acid, and Glucose-6-phosphate.

All buffers were 100 mM, except formic acid: 150 mM and Glucose-6-phosphate: 60 mM.

Sample preparation:
Individual samples for each buffer were adjusted to the desired pH values using $HCl_{(aq)}$ or $NaOH_{(aq)}$ until the desired pH was reached. The pH was measured using a Mettler Toledo SevenEasy S20 pH Meter, freshly calibrated. 10 v/v% DMSO was added to the samples to ensure dye solubility, and a final concentration of dye of ~5 μM was achieved by adding a small volume from the stock solution.
After spectroscopic measurements, the pH was measured to account for the pH change DMSO introduces. This pH value was used for data analysis.

Spectroscopy:
All measurements, except for the transient absorption samples, were performed in 1 cm path length UV Quartz cuvettes, with an absorbance below 0.1 for the $S_0 \rightarrow S_1$ transition.

UV/Vis absorption spectra were acquired using either a Cary 300 UV-Vis double beam spectrophotometer (Agilent Technologies) or a Lambda1050 UV/Vis/NIR double beam spectrophotometer (PerkinElmer). Air was used as the reference, and for baseline was a spectrum of the pure solvent for each sample measured.
Emission spectra were recorded on a PTI QuantaMaster8075 system (Horiba Scientific) or a FluoTime 300 system (PicoQuant) with a hybrid PMT detector, using a xenon lamp for excitation. Excitation spectra were measured using the PTI QuantaMaster8075 system.
All excitation and emission spectra were corrected for the xenon lamp profile and wavelength-dependent detector response.

The fluorescence decays were measured using time-correlated single photon counting (TCSPC) on the FluoTime 300 system. Samples were excited using pulsed laser excitation with either a 531 nm (LDH-D-TA-530B) solid-state laser or a 561 nm (LDH-D-TA-560) solid-state laser and the emission monochromator was set to 600 nm. For all samples data were collected until 10^4 counts were reached for the first time channel.

Decays were analyzed using the FluoFit software package (PicoQuant), to obtain the fluorescence lifetime. Where the decay ($I_f(t)$) was fitted by iterative reconvolution with a sum of exponentials:

$$I_f(t) = \sum a_i \exp\left(-\frac{t}{\tau_i}\right).$$

Here a_i is the amplitude and τ_i is the fluorescence lifetime of the i-th component. The instrument response function (IRF) was recorded using a dilute Ludox sample with the emission monochromator set to the excitation wavelength. The angle between the excitation and emission polarizers for all fluorescence measurements was set to magic angle (54.7°).
All samples were fitted using a monoexponential function until at high pH, when more than 95 % or more of the dyes are deprotonated, and required a bi-exponential fit.

For transient absorption (TA), the samples had an absorption of ~0.25 in a 1 mm quartz cuvette. The fs-Transient absorption experiments were performed using a femtosecond pump-probe setup. Laser pulses (796 nm, 60 fs pulse length, 4 kHz repetition rate) were generated by a regenerative amplifier (Solstice Ace) seeded by a femtosecond oscillator (Mai Tai SP, both Spectra Physics). For the pump a Topas C (Light Conversion) was used to obtain pulses with central wavelength located at 530 nm. Pump pulse energy was set to 0.5 μJ per pulse. The spot size was approximately 0.2 mm^2. For the probe the super-continuum generation from a thin CaF_2 plate was used. The mutual polarization between pump and probe beams was set to the magic angle (54.7°) by placing a Berek compensator in the pump beam. Prior to and following the fs-TA measurement, the steady-state absorption of the sample confirmed no laser-induced damage.

§2. Characterization of phenol-DAOTA and anisole-DAOTA

Table S1. Absorption maxima (λ_{max}) of the protonated (phenol-DAOTA, PhOH) and deprotonated (phenolate-DAOTA, PhO^-) form of the probe in different buffer systems, and the pK_a value of the probe determined in these solutions.

	Concentration (mM)	λ_{max} (PhOH) (nm)	λ_{max} (PhO^-) (nm)	pK_a
Acetic acid	100	557	560	8.9
Valine	100	557	560	8.9
Glutamic acid	100	557	560	8.9
Ethanolamine	100	557	560	8.8
Water		557	560	8.9
Phosphate	100	557	560	8.9
Phosphate & NaCl	Phosphate: 100 NaCl: 150	557	561	8.9
Formic acid	150	557	N/A	N/A
Glucose-6-phosphate	60	557	560	8.9
Glutamic acid in D_2O	100	556	560	9.25

Table S2. Absorption maxima of reference compound, anisole-DAOTA, in different buffer systems.

	Concentration (mM)	λ_{max} (nm)	τ_{acidic} (ns)	τ_{basic} (ns)
Phosphate	100	557	14.09	14.02
Glutamic acid	100	557	14.07	14.11
Ethanolamine	100	557	14.01	14.03
Acetate	100	557	14.18	14.19

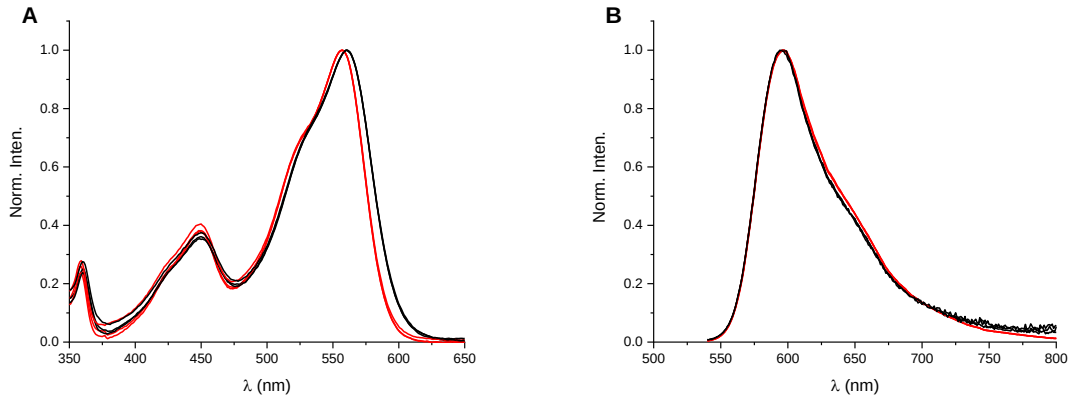

Figure S1. A) Normalized absorption spectra of phenol-DAOTA in three different buffers (100 mM); acetate, valine, and glutamic acid, under acidic conditions, pH ≈ 1 (red), and alkaline conditions pH ≈ 11-12 (black). B) Normalized emission spectra in the same buffers.

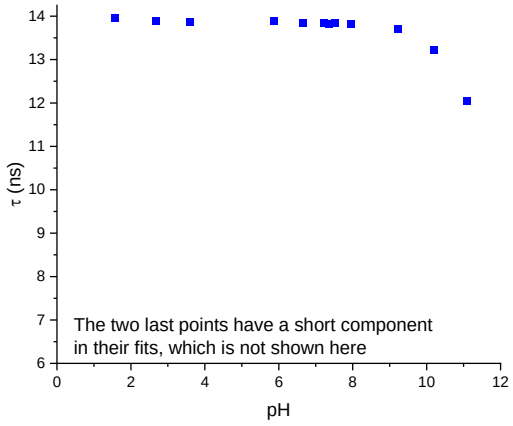

Figure S2. Fluorescence lifetime in water of phenol-DAOTA. At pH ≈ 10 and above, a bi-exponential fitting function is used in order to accurately fit the decay. The second component (not shown) is extremely short and is probably due to scattering.

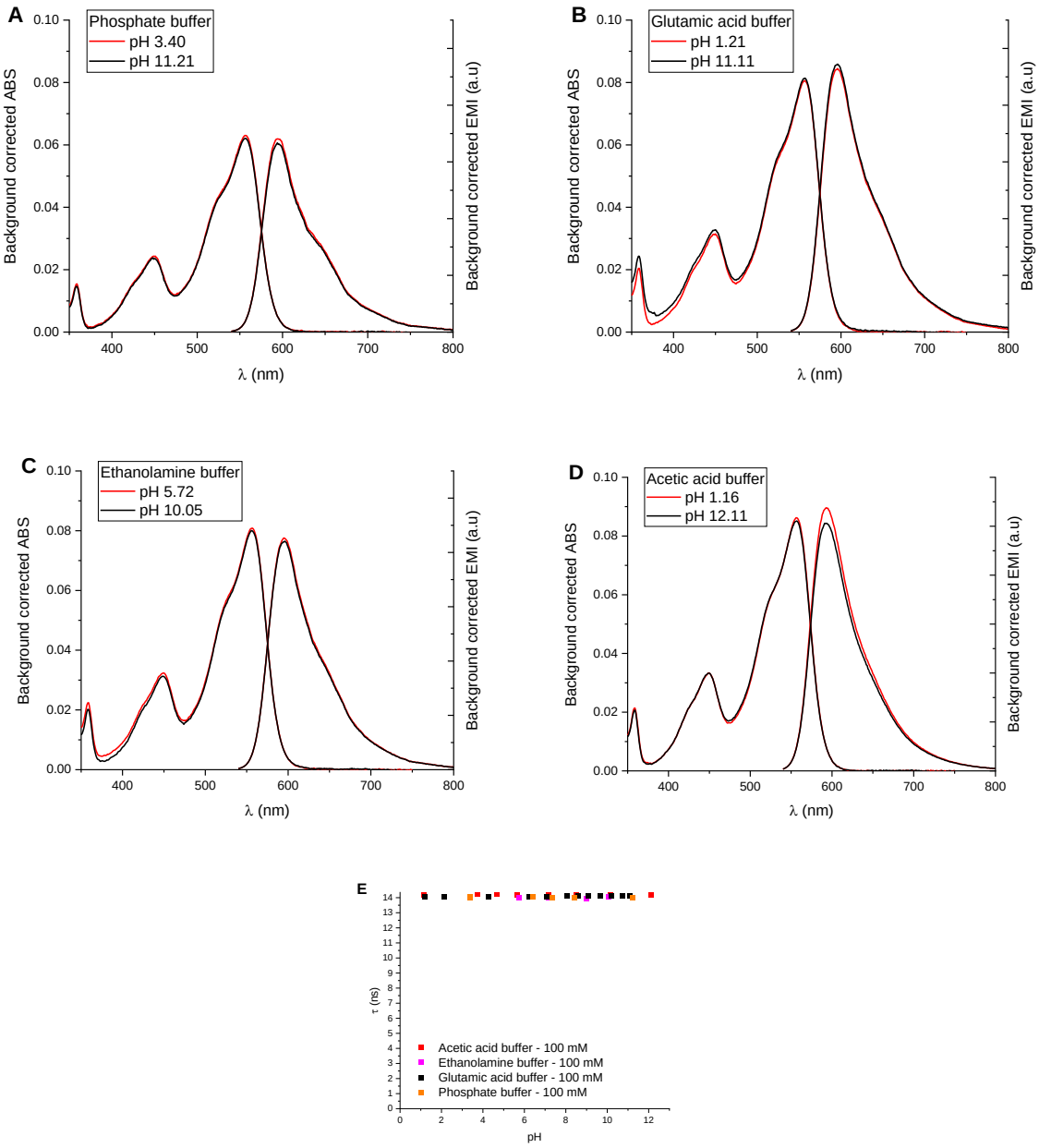

Figure S3. A-D) Absorption and emission spectra of anisole-DAOTA in different buffers (100 mM): phosphate (PB), Glutamic acid, ethanolamine, and acetate. Red: acidic pH, black: alkaline pH. Exact pH values given in legends. E) Fluorescence lifetime from mono-exponential fits to the fluorescence decays in the abovementioned buffers.

§3. Determination of PET rate in phenolate-DAOTA

The PET rate was investigated using transient absorption in acetonitrile with 10 v% water. The deprotonated fluorophore was measured, where approximately 1.5 v% 0.1 M NaOH solution was added to the sample. Complete deprotonation under these conditions was confirmed by absorption and fluorescence spectroscopy showing expected $\lambda_{max,abs}$ shift and full quenching, respectively. Femtosecond transient absorption spectra are shown in Figure S4. As expected, no change in the TA spectra is observed on the experimental timescale for the protonated fluorophore: phenol-DAOTA, due to its long fluorescence lifetime ($\tau \approx 17$ ns in this solvent mixture) (Figure S4 left). For the deprotonated form: phenolate-DAOTA, the ESA signal around 400 nm and the GSB around 580 nm show fast decay and recovery respectively.

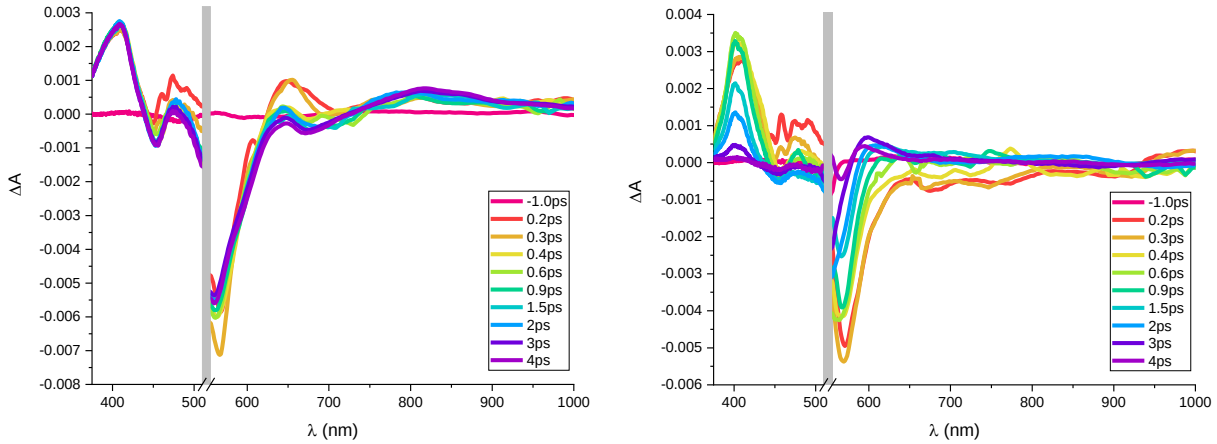

Figure S4. Transient absorption data of left) phenol-DAOTA and right) phenolate-DAOTA. Both show ESA around 400 nm and GSB around 580 nm with significantly different timescales.

The ESA at around 400nm of phenolate-DAOTA (Figure S5A) display a slow build-up process, slower than the instrument response function (IRF, ~100 fs). The slow build-up process is accompanied by a shift in the spectra at around 420 nm. The build-up process of the GSB signal at around 580 nm is however at the same timescale as the IRF (Figure S5B). The kinetics of the signal at 400 nm and 580 nm were analyzed by deconvolution fit with IRF. For phenolate-DAOTA, the fit considers both build-up and decay processes, which are shown in Figure S5C. For phenol-DAOTA, the fit only considers the build-up process as shown in Figure S5D as the excited-state lifetime of phenol-DAOTA is longer than the fs-TA measurement time window.

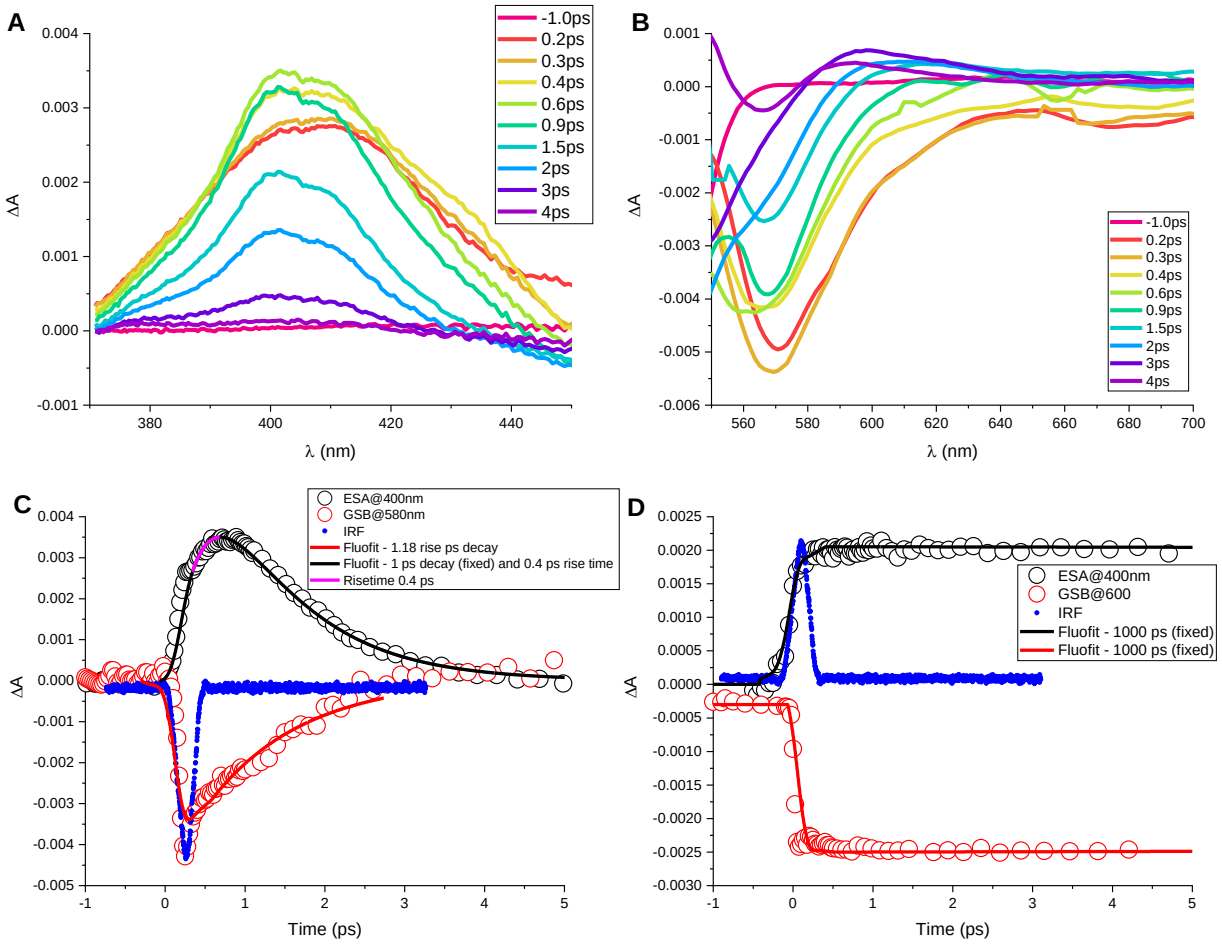

Figure S5. TA data for phenolate-DAOTA and phenol-DAOTA. A) Zoom in on the ESA spectra for phenolate-DAOTA, where a fast and a slower rise time is observed. B) The GSB around 580 nm for phenolate-DAOTA. C) and D) Deconvoluted fits for ESA and GSB for phenolate-DAOTA and phenol-DAOTA, respectively. Phenol-DAOTA shows no decay on this short time scale, according to its long fluorescence lifetime.

For phenolate-DAOTA, the recovery time constant of the GSB signal was obtained by fitting the data from -1 ps to approximately 2.5 ps. The recovery process of the GSB signal could in this range be fitted with a single decay component of 1.18 ps. The rest of the data was not used due to the noise. A similar deconvolution fitting approach was used to obtain the build-up time of the ESA at 400 nm. To obtain an accurate rise time, a 1 ps decay time was fixed in the fitting procedure whereby a 400 fs build-up time could be resolved (highlighted in pink).

For phenol-DAOTA, Figure S5D, both the ESA and GSB signals build up instantaneously, and the ESA is here assigned to the FC state, which is the first excited-state (S_1).

From the deconvolution fit results, we can conclude that the PET process has a timescale of about 400 fs and that the decay timescale of the PET state is about 1 ps. The fast formation and decay of the PET state explain its efficient fluorescence quenching, and it also supports the model in which deprotonation in the excited state always leads to PET quenching without re-protonation occurring.

§4. pH response of phenol-DAOTA in buffer solutions

Between 10 to 17 samples with different pH were prepared for each buffer system. The absorption, emission, and fluorescence decay were measured for each of these samples, and the data was then analyzed as described below.

The ground state pK_a of phenol-DAOTA was in each case obtained from the normalized absorption spectra. The pH response was quantified by numerical integration of the red-edge (570-620 nm). The obtained values were scaled to the range between 0 to 1 (A_{int}) and plotted as a function of pH. A theoretical Henderson-Hasselbalch (HH) equation was then applied to match the data [Eq. 1]:

$$A_{int}(pH) = \frac{1}{10^{pK_{a,phenol-DAOTA}-pH} + 1}. \qquad Eq.\,1$$

The pK_a of phenol-DAOTA was found to be 8.9 in all the buffers (Table S1).

The fluorescence lifetime values (obtained from fitting single exponential functions to the intensity decays) were plotted as a function of pH and fitted using a theoretical HH function [Eq. 2]:

$$\tau(pH) = \tau^0 \times \left(\sum_{i=1}^{n} \left(p_{\tau,i} \times \frac{1}{10^{pH-pK_{a,i}} + 1} \right) + \left(1 - \sum_{i=1}^{n} p_{\tau,i} \right) \right). \qquad Eq.\,2$$

Here τ^0 is the fluorescence lifetime of the most acidic sample i.e. the unquenched phenol-DAOTA, and $p_{\tau,i}$ is the percentile decrease the buffer introduces at $pK_{a,i}$, where n is the number of pK_a values in the buffer. In this equation, the only changeable parameter is $p_{\tau,i}$. The $p_{\tau,i}$ value can most often be estimated from the ratio between the fluorescence lifetime at the plateaus before and after a decrease at $pK_{a,i}$. For buffers with $pK_a \geq pK_{a,phenol-DAOTA}$, the decrease in the fluorescence lifetime might not converge towards a plateau within the range where reliable lifetimes can be measured, and the $p_{\tau,i}$ value which fitted the data the best was used.

The pH response for the emission spectra is observed as an intensity decrease. The emission maximum for each sample was normalized relative to the most fluorescent sample (most acidic pH) and plotted as a function of pH (I_f). A theoretical HH equation was then superimposed on the data [Eq. 3]:

$$I_f(pH) = \frac{1}{10^{pH-pK_{a,phenol-DAOTA}} + 1}. \quad Eq.3$$

When measured in buffers with pK_a value(s) below that of phenol-DAOTA, additional intensity decrease(s) can be observed, corresponding to the dynamic PCET quenching promoted by the base components in the buffer. To account for the additional decrease(s) in I_f extra terms in the HH equation were added [Eq. 4]:

$$I_f(pH) = \left(\sum_{i=1}^{n} p_{I,i} \times \frac{1}{10^{pH-pK_{a,i}} + 1}\right) + \left(\left(1 - \sum_{i=1}^{n} p_{I,i}\right) \times \frac{1}{10^{pH-pK_{a,phenol-DAOTA}} + 1}\right). \quad Eq.4$$

Here $p_{I,i}$ is the percentile decrease introduced by the base in the buffer with the specific $pK_{a,i}$ value, and n is the total number of pK_a value(s) below $pK_{a,phenol-DAOTA}$. The initial value for each $p_{I,i}$ is estimated from the $p_{\tau,i}$ obtained from the fluorescence lifetime analysis. The $p_{I,i}$ values was then optimized to obtain best correspondence. Comparison of the drop in lifetime and intensities are compiled in Table S4.

In the HH functions applied above, the pK_a value(s) used in the data analysis are literature values of the buffers, with minor differences for the glucose-6-phosphate and formic acid buffers (see Figures S13-14). Literature values are listed in Table S3.

Table S3. Literature pK_a values, all obtained from CRC handbook of chemistry and physics 75th edition, unless otherwise stated.[2]

Buffers investigated	pK_a values	Titration data in Figure
Acetic acid	4.76	S6
Valine	2.29 & 9.74	S7
Glutamic acid	2.19, 4.25, & 9.67	S8
Ethanolamine	9.5	S9
Water	14	S10
Phosphate (0.1 M) [a]	2.1 & 6.8	S11 S12 (with 150 mM NaCl)
Formic acid	3.75	S13
Glucose-6-phosphate [b]	0.94-1.65 & 6.11-6.22	S14

[a]The second pK_a in a 0.1 M phosphate buffer was fitted to 6.8 instead of 7.2 due to the increased ionic strength.[3-4] [b]Different pK_a values are reported in the literature.[4-6]

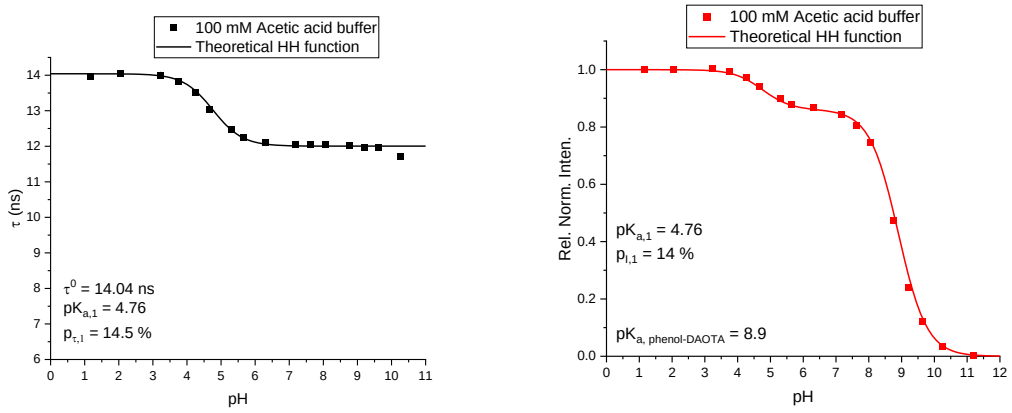

Figure S6. Phenol-DAOTA in 100 mM acetate buffer with pK_a 4.76.
Left) Fluorescence lifetime values as a function of pH.
Right) Relative fluorescence intensity as a function of pH.
Lines are theoretical HH functions fitted to the experimental data with parameters in the corners.

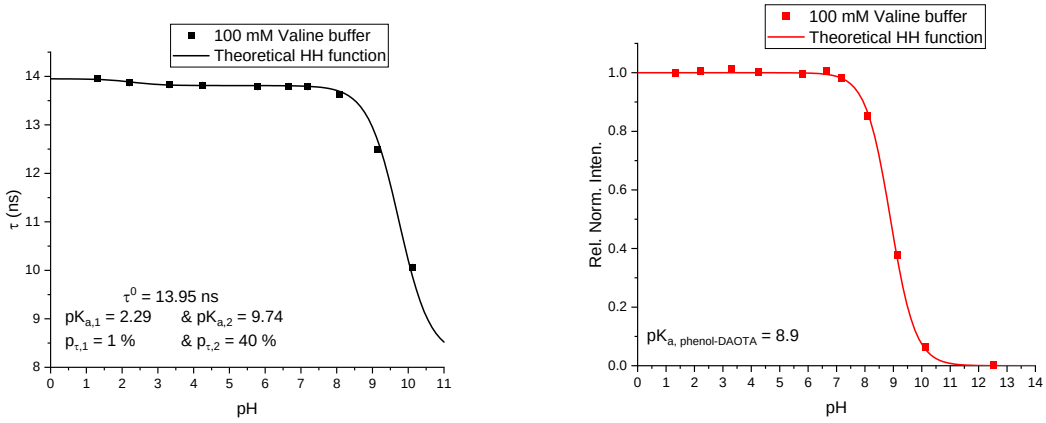

Figure S7. Phenol-DAOTA in 100 mM valine buffer with pK_a 2.29 & 9.74.
Left) Fluorescence lifetime values as a function of pH.
Right) Relative fluorescence intensity as a function of pH.
Lines are theoretical HH functions fitted to the experimental data with parameters in the corners.

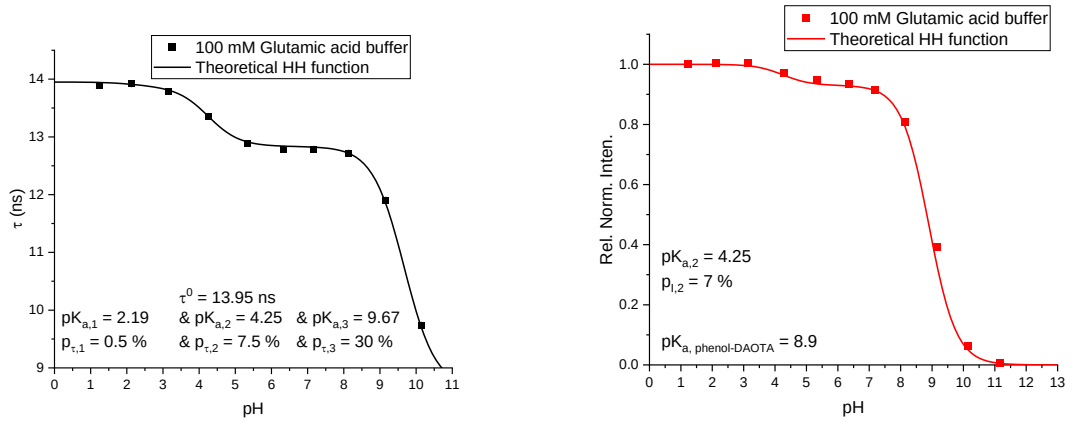

Figure S8. Phenol-DAOTA in 100 mM Glutamic acid buffer with pK_a 2.19, 4.25, & 9.67.
Left) Fluorescence lifetime values as a function of pH.
Right) Relative fluorescence intensity as a function of pH.
Lines are theoretical HH functions fitted to the experimental data with parameters in the corners.

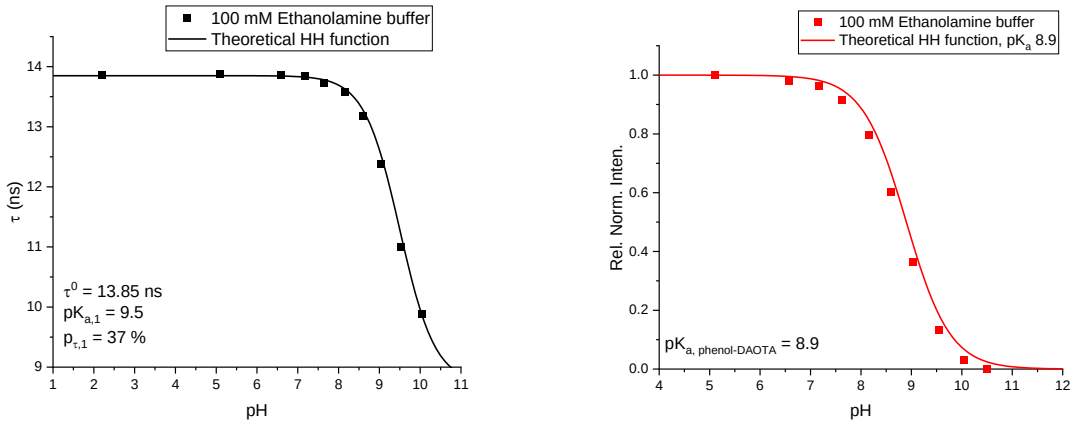

Figure S9. Phenol-DAOTA in 100 mM ethanolamine buffer with pK_a 9.5.
Left) Fluorescence lifetime values as a function of pH.
Right) Relative fluorescence intensity as a function of pH.
Lines are theoretical HH functions fitted to the experimental data with parameters in the corners.
The quenching of the fluorescence intensity is only due to deprotonation in the ground state.

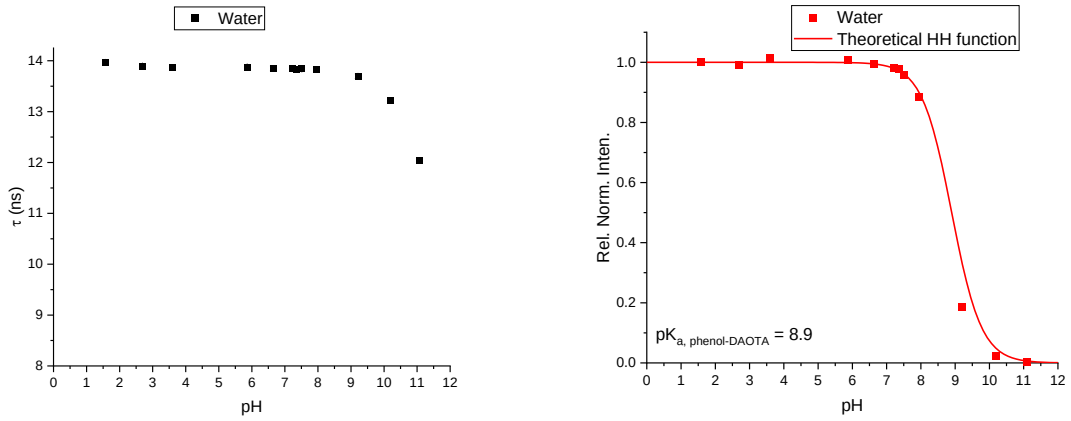

Figure S10. Phenol-DAOTA in water.
Left) Fluorescence lifetime values as a function of pH. The two last fluorescence lifetimes are the longest component from a biexponential fit
Right) Relative fluorescence intensity as a function of pH.
Line is a theoretical HH function fitted to the experimental data with parameter in the corners.
The quenching of the fluorescence intensity is only due to deprotonation in the ground state.

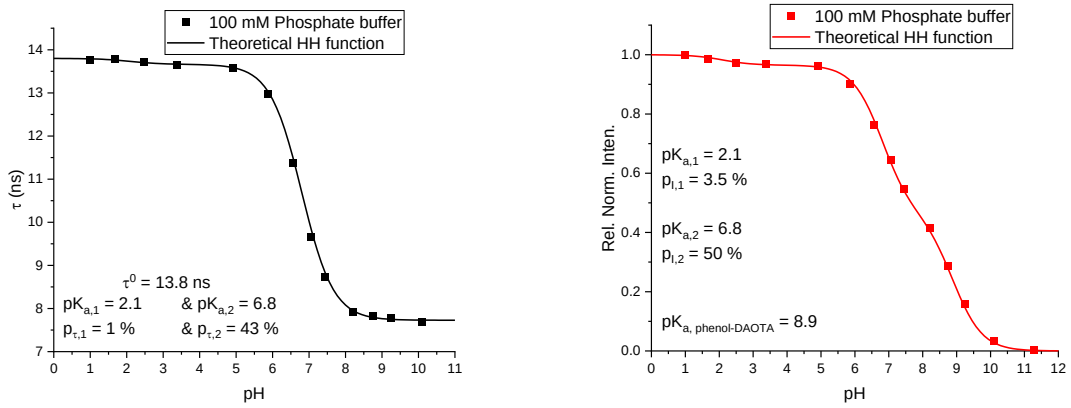

Figure S11. Phenol-DAOTA in 100 mM phosphate buffer with pK_a 2.1 & 6.8.
Left) Fluorescence lifetime values as a function of pH.
Right) Relative fluorescence intensity as a function of pH.
Lines are theoretical HH functions fitted to the experimental data with parameters in the corners.

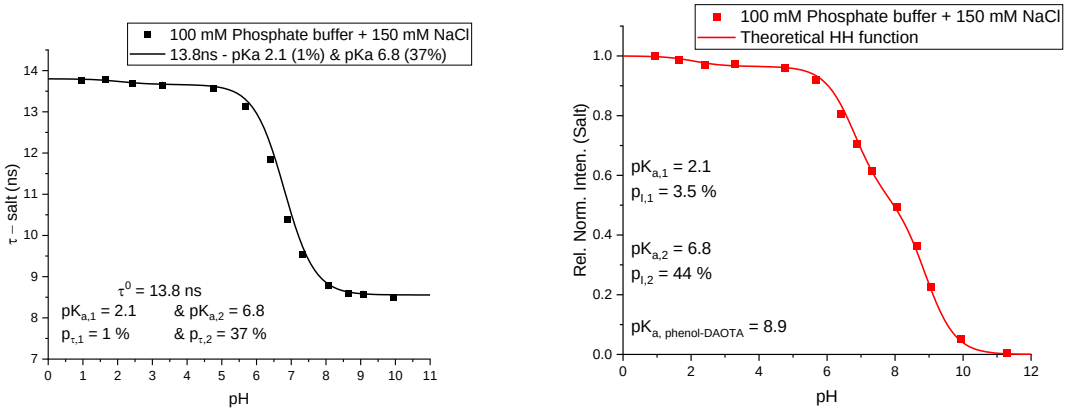

Figure S12. Phenol-DAOTA in 100 mM phosphate buffer and 150 mM NaCl with pK_a 2.1 & 6.8.
Left) Fluorescence lifetime values as a function of pH.
Right) Relative fluorescence intensity as a function of pH.
Lines are theoretical HH functions fitted to the experimental data with parameters in the corners.

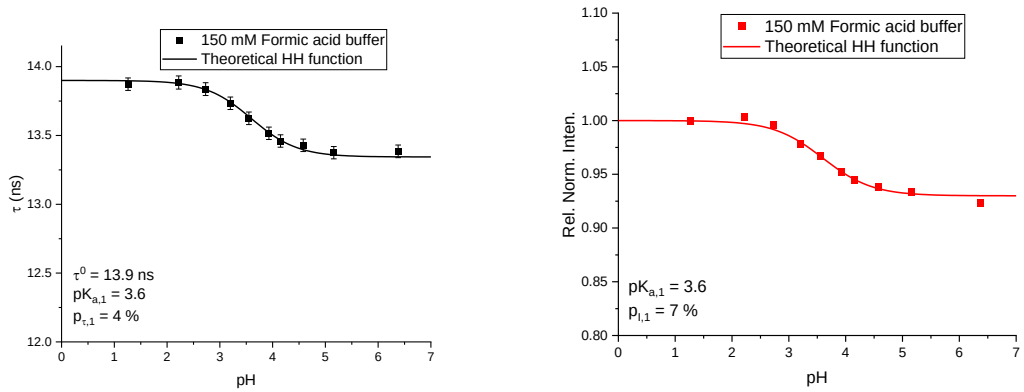

Figure S13. Phenol-DAOTA in 150 mM formic acid buffer with pK_a 3.6.
Left) Fluorescence lifetime values as a function of pH.
Right) Relative fluorescence intensity as a function of pH.
Lines are theoretical HH functions fitted to the experimental data with parameters in the corners.

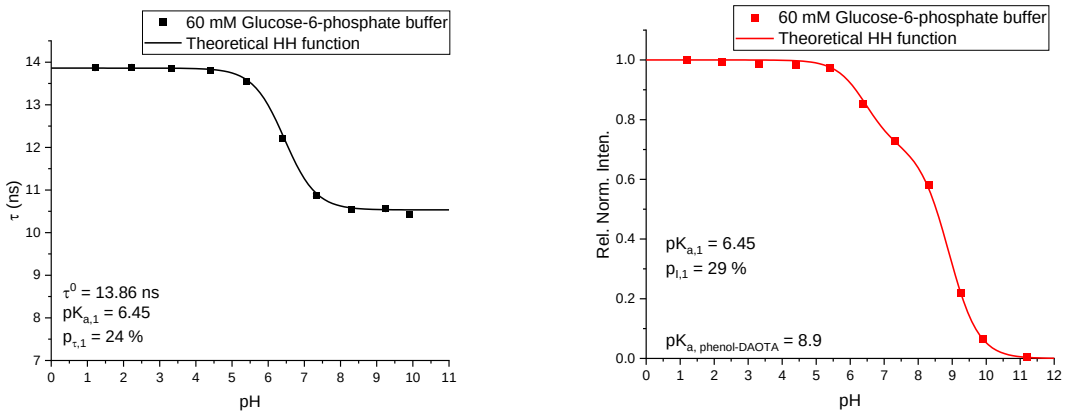

Figure S14. Phenol-DAOTA in 60 mM glucose-6-phosphate buffer with pK_a 6.45.
Left) Fluorescence lifetime values as a function of pH.
Right) Relative fluorescence intensity as a function of pH.
Lines are theoretical HH functions fitted to the experimental data with parameters in the corners.

Table S4. Comparison of the decrease in fluorescence lifetime and fluorescence intensities in different buffer systems.

	Concentration (mM)	pK_a	τ^0 (ns)	$\Delta\tau$ %	ΔI %	Figure
Acetic acid	100	4.76	14.04	14.5	14	S6
Valine	100	2.29 9.74	13.95	1 40		S7
Glutamic acid	100	2.19 4.25 9.67	13.95	0.5 7.5 30	7	S8
Ethanolamine	100	9.5	13.85	37		S9
water	-		13.97	-	-	S10
Phosphate	100	2.1 6.8	13.76	1 43	3.5 50	S11
Phosphate & NaCl	100 NaCl 150	2.1 6.8	13.76	1 37	3.5 44	S12
Formic acid	150	3.6	13.87	4	7	S13
Glucose-6-phosphate	60	6.45	13.86	24	29	S14

§5. Stern-Volmer analysis of the fluorescence lifetime data

The fluorescence lifetime for each buffer was further analyzed using Stern-Volmer analysis:

$$\frac{\tau^0}{\tau} = 1 + \tau^0 k_{\mathrm{PCET}}[B:], \qquad Eq.\,5$$

where τ^0 is the fluorescence lifetime of the probe without the base present, k_{PCET} is the rate of base assisted proton transfer experienced by the excited probe, and $[B:]$ is the concentration of the base. $[B:]$ is calculated from the HH equation using the pK_a of their corresponding acid, the pH in the solution and the total buffer concentrations. The value of k_{PCET} can be obtained from the slope of the linear fit(s).

For buffer systems with more than one pK_a values in the pH range investigated, each corresponding base was analyzed individually. Hence, each decrease from one plateau to the next plateau, the effect of the increased base concentration, has been analyzed individually. The τ^0 for each analysis was taken from the fluorescence lifetime of the most acidic sample in the last plateau regime.

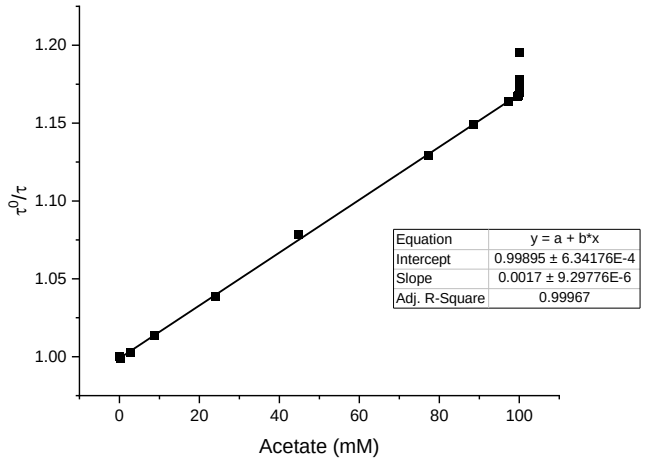

Figure S15. Stern-Volmer plot of Phenol-DAOTA in 100 mM acetic acid buffer with pK_a 4.76. The fit was only taken between pH=1 to pH=8, as the fluorescence lifetime values above 8 includes the effect of hydroxide ions in solution, leading to an increase in the τ^0/τ value.

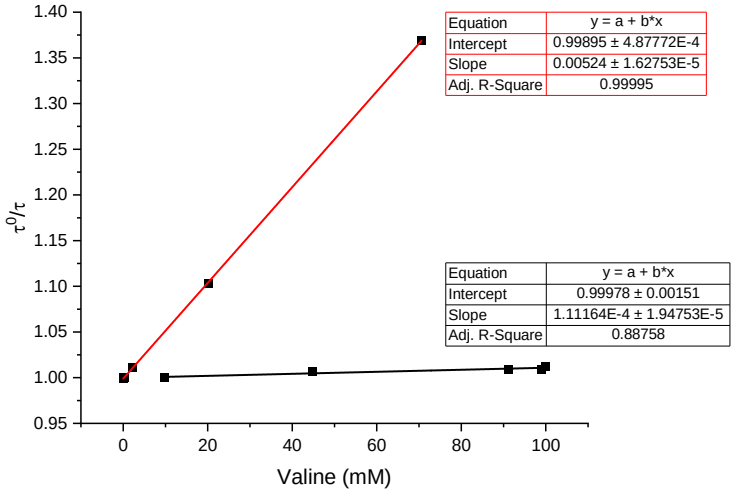

Figure S16. Stern-Volmer plot of Phenol-DAOTA in 100 mM valine buffer with pK_a 2.29 & 9.74.

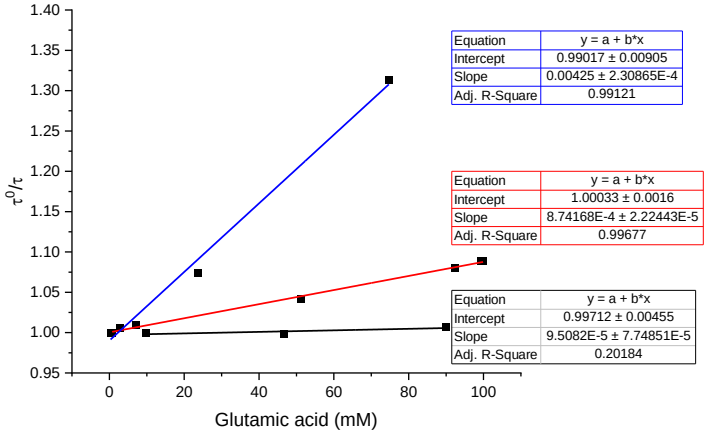

Figure S17. Stern-Volmer plot of Phenol-DAOTA in 100 mM glutamic acid buffer with pK_a 2.19, 4.25, & 9.67.

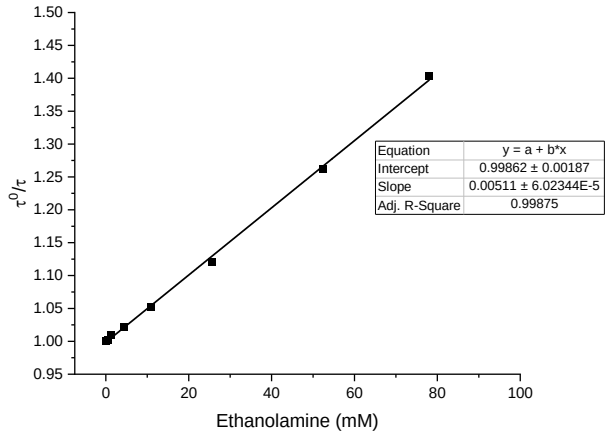

Figure S18. Stern-Volmer plot of Phenol-DAOTA in 100 mM ethanolamine buffer with pK_a 9.5.

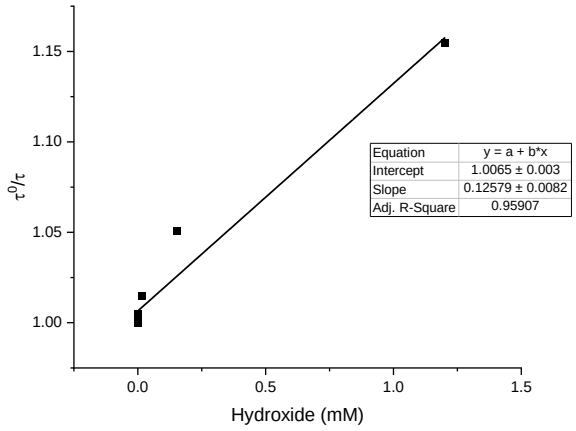

Figure S19. Stern-Volmer plot of Phenol-DAOTA in water with pK_a 14.

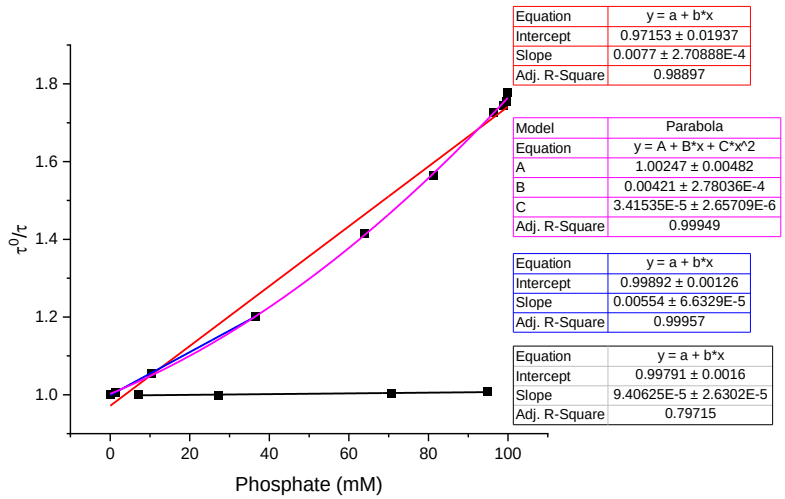

Figure S20. Stern-Volmer plot of Phenol-DAOTA in 100 mM phosphate buffer with pK_a 2.1 & 6.8. A linear fit (red) of all the data points for pK_a 6.8 does not fit the data well, only up to around 40 mM of HPO_4^{2-}. A second order fit (purple) does however seem to fit the data, illustrating the increased quenching effect form this buffer at high concentrations.

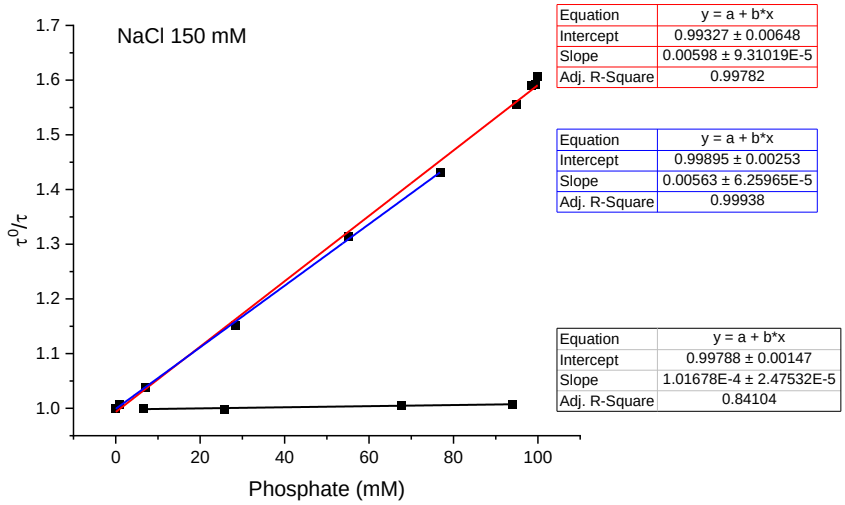

Figure S21. Stern-Volmer plot of Phenol-DAOTA in 100 mM phosphate buffer and 150 mM NaCl with pK_a 2.1 & 6.8. A linear fit now fits almost all data points for pK_a 6.8, but the fit up to only 80 mM (blue) has been used in calculated k_{PCET}.

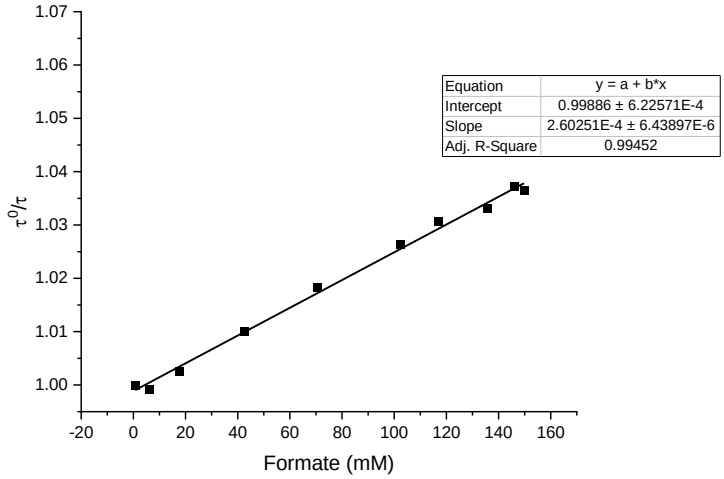

Figure S22. Stern-Volmer plot of Phenol-DAOTA in 150 mM formic acid buffer with pK_a 3.6.

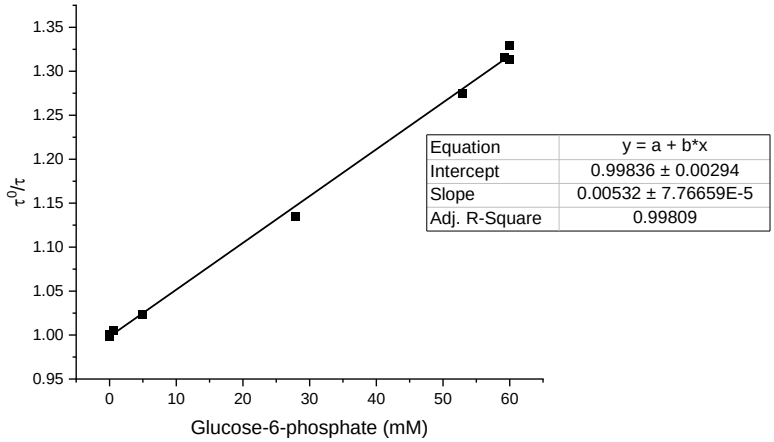

Figure S23. Stern-Volmer plot of Phenol-DAOTA in 60 mM glucose-6-phosphate buffer with pK_a 6.45.

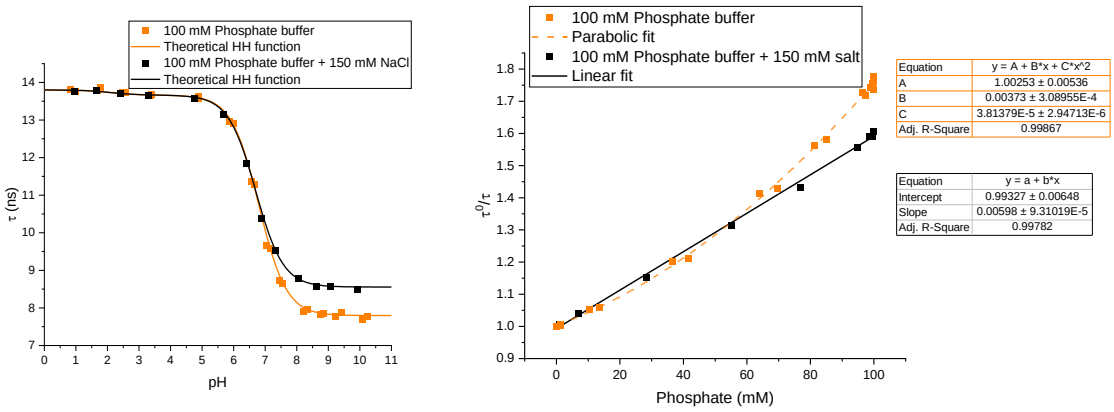

Figure S24. Comparison of Phenol-DAOTA in 100 mM phosphate buffer with pK_a 6.8, with and without NaCl.

Left) Fluorescence lifetime values as a function of pH with a theoretical HH function superimposed of samples with (black) and without salt (orange). The fluorescence lifetime is less quenched when salt is added by 6 %.

Right) Stern-Volmer analysis of samples with (black) and without NaCl (orange). The solution with salt can be fitted relatively well with a linear fit following a standard dynamic quenching process, whereas the samples without salt requires a parabola to accurately fit the data at high hydrogen phosphate concentrations.

Table S5. Proton coupled electron transfer rate constants for each base in the investigated buffers. The value for phosphates are including NaCl and for HPO_4^{2-} is the linear part only from 0 to 80 mM.

	pK_a (conjugated acid)	ΔpK_a (Acceptor – Donor)	k_{PCET} (M^{-1} s^{-1}) ($\times 10^7$)	Log (k_{PCET})
Acetic acid	4.76	-4.14	12	8.07
Valine (Val)	2.29	-6.61	0.8	6.9
Valine (Val^-)	9.74	0.84	38	8.58
Glutamic acid (Glu^0)	2.19	-6.71	0.7	6.84
Glutamic acid (Glu^-)	4.25	-4.65	6.3	7.8
Glutamic acid (Glu^{2-})	9.67	0.77	33	8.52
Ethanolamine (ETA)	9.5	0.6	37	8.57
Hydroxide (OH^-)	14	5.1	>900	9.96
Phosphate ($H_2PO_4^-$)	2.1	-6.8	0.8	6.88
Phosphate (HPO_4^{2-})	6.8	-2.1	41	8.62
Formic acid (HCO_2^-)	3.6	-5.3	1.9	7.27
Glucose-6-phosphate ($G6P^{2-}$)	6.45	-2.45	39	8.59

§6. Comparison with phenol and diffusion correction

Proton transfer from phenol to various bases have previously been studied by Eigen and Bell.[7-8] They reported a maximum log(k_{PCET}) ≈9.3, which is one order of magnitude larger than the values found with phenol-DAOTA. This we attribute to the faster diffusion of the smaller phenol molecule compared to phenol-DAOTA. To achieve a better basis for comparison, the k_{PCET} values were corrected taking the difference in diffusion rates into account.

$$k_{\mathrm{PCET},\ diffusion\ corrected} = k_{\mathrm{PCET}}\left(\frac{D_B + D_{phenol}}{D_B + D_{DAOTA}}\right)$$

Here D_B is the diffusion constant of the base, D_{phenol} and D_{DAOTA} the diffusion constant of the phenol and phenol-DAOTA respectively. For phenol and phenol-DAOTA, the diffusion constant was calculated using the Stokes-Einstein equation assuming spherical molecules $D = \frac{k_B T}{6\pi r \eta_0}$.

The radius (r) of the molecules was estimated from the molecular mass and assuming a density of 1g/cm^3.

Table S6. Estimated diffusion constants for phenol and phenol-DAOTA.

Proton donor	Molar mass (g/mol)	Radius $\times 10^{8}$ (cm)	Diffusion constant $\times 10^{-6}$ (cm^2/s)
Phenol	94.11	3.3	6.4
Phenol-DAOTA	389.43	5.4	4.0

Table S7. Literature diffusion constants from CRC handbook of chemistry and physics 75th edition[9] unless otherwise stated and log(k_{PCET}) and log($k_{PCET,\ diffusion\ corrected}$) values.

Buffer	Diffusion rate $\times 10^{-6}$ (cm^2/s)	log(k_{PCET})	log($k_{PCET,\ diffusion\ corrected}$)
Acetic acid	10.89	8.07	8.68
Valine[a]	7.725	6.90, 8.58	7.61, 9.28
Glutamic acid[a.b]	7.623	6.84, 7.80, 8.52	7.54, 8.50, 9.23
Ethanolamine	10.8	8.57	9.17
Hydroxide	52.73	9.96	9.97
Phosphate[c]	8.79	6.88, 8.62	7.5, 9.28
Formic acid	14.54	7.27	7.78
Glucose-6-phosphate[d]	6.7	8.59	9.34

[a]From Longsworth.[10] [b]Diffusion constant reported for glutamine. [c]Diffusion constant reported for $H_2PO_4^-$ (aq.). [d]Diffusion constant reported for glucose.

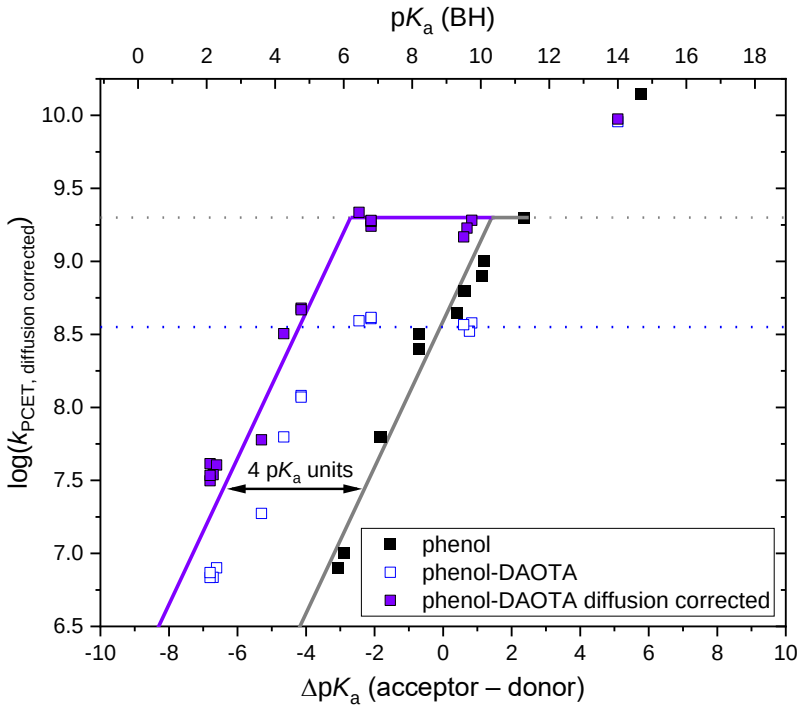

Figure S25. Quenching rate k_{PCET} as a function of ΔpK_a for phenol-DAOTA, diffusion corrected (purple squares), phenol from Bell and Eigen (black squares) and original non-corrected values phenol-DAOTA (blue open squares).

§7. Note on uncertainties and repeatability of the measurements

The variability of the measurement data will mainly be due to uncertainties in the buffer preparation, pH-meter and fits of the fluorescence decays in the lifetime measurements.

The lifetime measurements and analysis performed here (see §1, spectroscopy) have a low standard deviation in the range of ~0.05 ns (see §8).

Figure S26 show the intensity and lifetime response of phenol-DAOTA in two independently prepared acetate buffers. The two measurements show good agreement, which demonstrates the reproducibility of the probe response and measurements.

Furthermore, some measurements such as the phosphate pH titration with and without NaCl, also show good repeatability of the measurements displaying the same probe response until the salt effect sets in (Figure S24). The mixed buffer experiment (See §10) also showcases the reliability of the system as the k_{PCET} rates found for the individual bases can be used to predict the total response in a mixture.

In addition, for all titration series the data points match theoretical Henderson-Hasselbalch curves using base pK_a values found in the literature, which again is a testament to the reliability of probe system, spectrometers and pH-meter measurement (See §4).

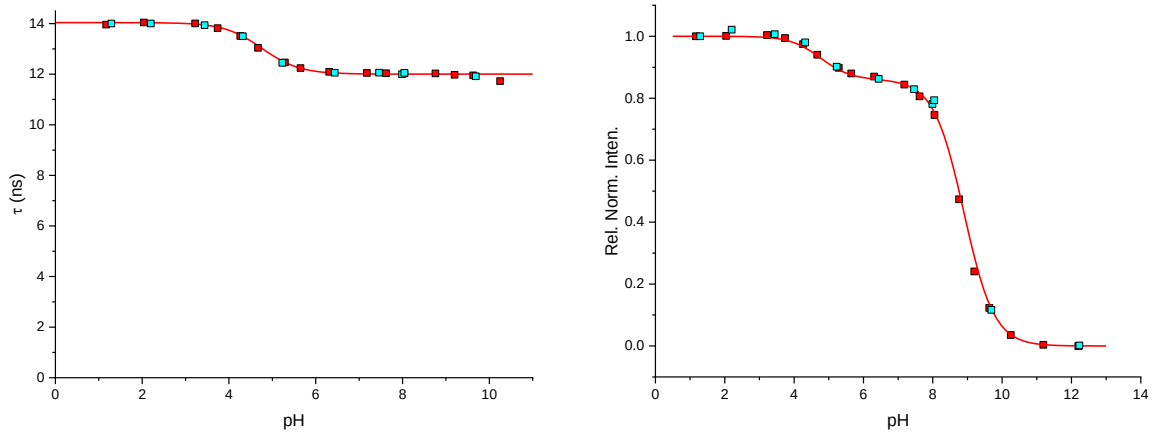

Figure S26. Response of Phenol-DAOTA measured in two different 100 mM acetate buffer with pK_a 4.76, shown in red and cyan.
Left) Fluorescence lifetime values as a function of pH.
Right) Relative fluorescence intensity as a function of pH.
Lines are theoretical HH functions fitted to the red experimental data.

§8. Calculation of limit of detection

The limit of detection (LOD) is calculated using the same method described by Jakobsen and Laursen.[11] The ratio between the unquenched lifetime (τ^0) and τ^0 substracted by 3 times the standard deviation (σ_{τ^0}) obtained from the fluorescence lifetime fit, was divided by the Stern-Volmer constants ($K_{SV} = k_{PCET} \times \tau^0$) found for each buffer.

$$LOD = \frac{\frac{\tau^0}{\tau^0 - 3 \cdot \sigma_{\tau^0}} - 1}{K_{SV}}$$

Table S8. Limit of detection calculated for formate, phosphate and acetate.

	τ^0 (ns)	σ_{τ^0} (ns)	K_{SV} (M^{-1})	LOD (mM)
Formate	13.87	0.0456	0.260	38.3
$H_2PO_4^-$ 150mM NaCl	13.76	0.046	0.102	99.7
HPO_4^{2-} 150 mM NaCl	13.76	0.046	5.98	1.69
Acetate	13.96	0.049	1.64	6.49

§9. Response of phenol-DAOTA in D_2O

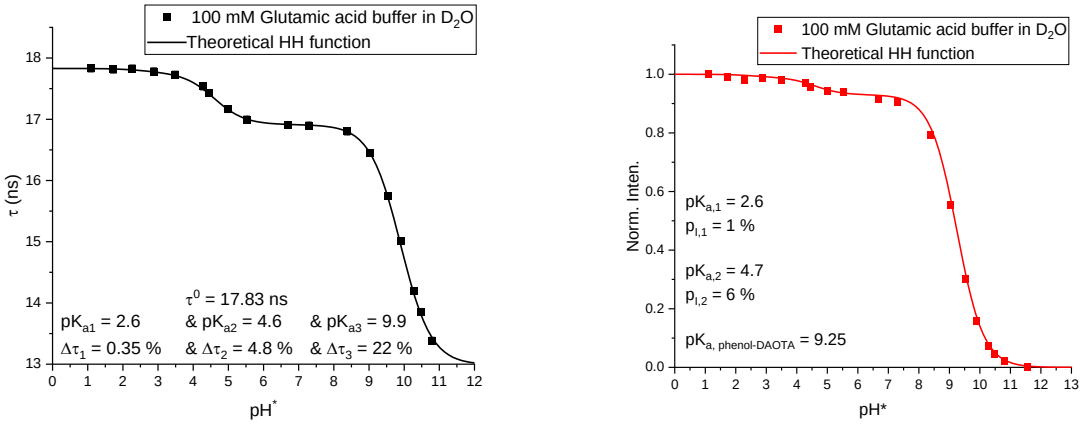

Figure S27. Phenol-DAOTA in 100 mM glutamic acid buffer in D_2O with pK_a 2.6, 4.6, & 9.9.
Left) Fluorescence lifetime values as a function of pH*.
Right) Relative fluorescence intensity as a function of pH*.

Lines are theoretical HH functions fitted to the experimental data with parameters in the corners.

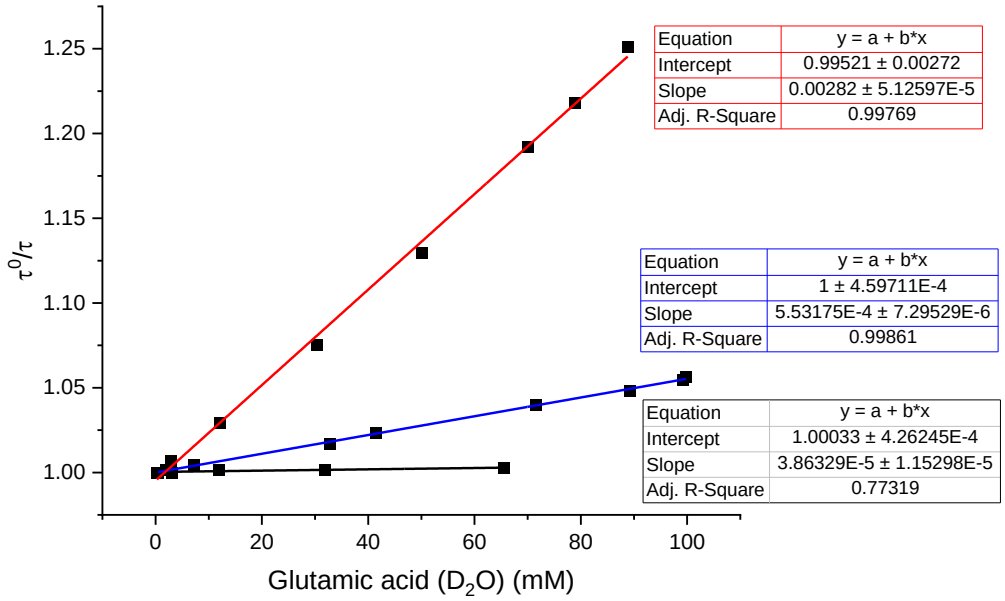

Figure S28. Stern-Volmer plot of Phenol-DAOTA in 100 mM glutamic acid buffer in D_2O with pK_a 2.6, 4.6, & 9.9.

Table S10. Kinetic isotope effect (KIE) comparison in glutamic acid buffers.

Glutamic acid	k_{PCET}(H) (M^{-1} s^{-1}) (×10^7)	k_{PCET}(D) (M^{-1} s^{-1}) (×10^7)	KIE k_{PCET}(H) / k_{PCET}(D)
Glu^0	0.68	0.23	2.9
Glu^-	6.28	3.03	2.1
Glu^{2-}	33.25	17.11	1.9

§10. pH response of phenol-DAOTA in a buffer mixture

The quenching rates (k_{PCET}) determined for the individual buffers (Table S5) can be used to calculate the response of the phenol-DAOTA in a buffer mixture as a function of the used bases (Q_i) and their concentrations (that in turn is a function of pH):

$$\tau = \frac{1}{\frac{1}{\tau^0} + k_{PCET}^{Q_1}[Q_1] + k_{PCET}^{Q_2}[Q_2] + \cdots + k_{PCET}^{Q_i}[Q_i]}$$

To demonstrate the response of the phenol-DAOTA, a mixed buffer system consisting of acetate 100 mM and phosphate 100 mM was prepared and pH adjusted as described above (see §1).

Figure S28 show the calculated fluorescence lifetime and experimentally measured fluorescence lifetimes as a function of pH. The measured fluorescence lifetimes correlate very well to the calculated lifetimes.

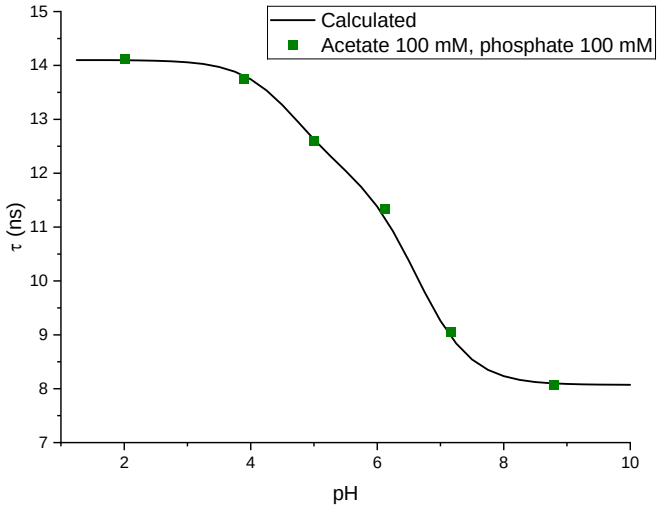

Figure S29. Phenol-DAOTA in a buffer of 100 mM acetate and 100 mM phosphate. Expected fluorescence lifetime as function of pH was calculated based on the quenching rates found in individual acetate and phosphate (with NaCl) buffers (black line). Experimental fluorescence lifetime values at six pH values are shown as green points.

§11. Elimination of "autofluorescence" by time-gating

In cellular and tissue environments, autofluorescence is a common phenomenon interfering with the probe signal. This affects both intensity measurements and fluorescence lifetimes. In this study, the long fluorescence lifetime of phenol-DAOTA gives the additional advantage of using time-gating to exclude the autofluorescence from the measurement.

To demonstrate this, a short lifetime cyanine dye, 3,3-Diethyloxadicarbocyanine iodide (DODC), with similar absorption and emission spectra to phenol-DAOTA (Figure S29) was used to simulate an autofluorescent environment. The fluorescence lifetime of phenol-DAOTA was measured in 100 mM phosphate buffer at acidic or basic conditions. The cyanine was then added to the cuvette and the lifetime measured again (Figure S30). The cyanine signal contributed ~7% and ~26% to the total intensity measured for the acidic and basic samples respectively.

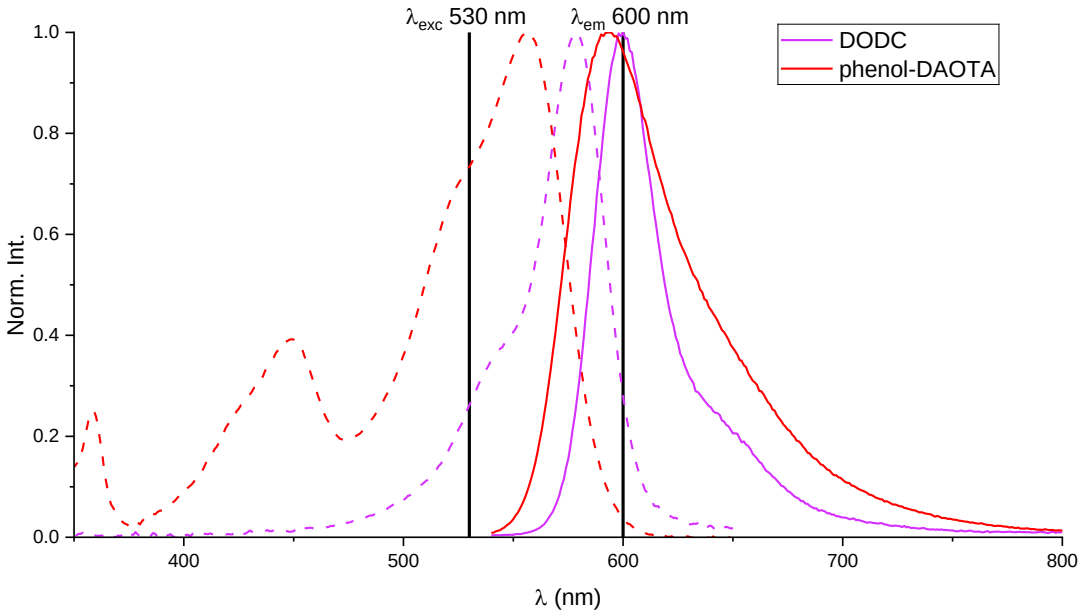

Figure S30. Normalized absorption and emission spectra of DODC and phenol-DAOTA with corresponding excitation and emission detection wavelengths.

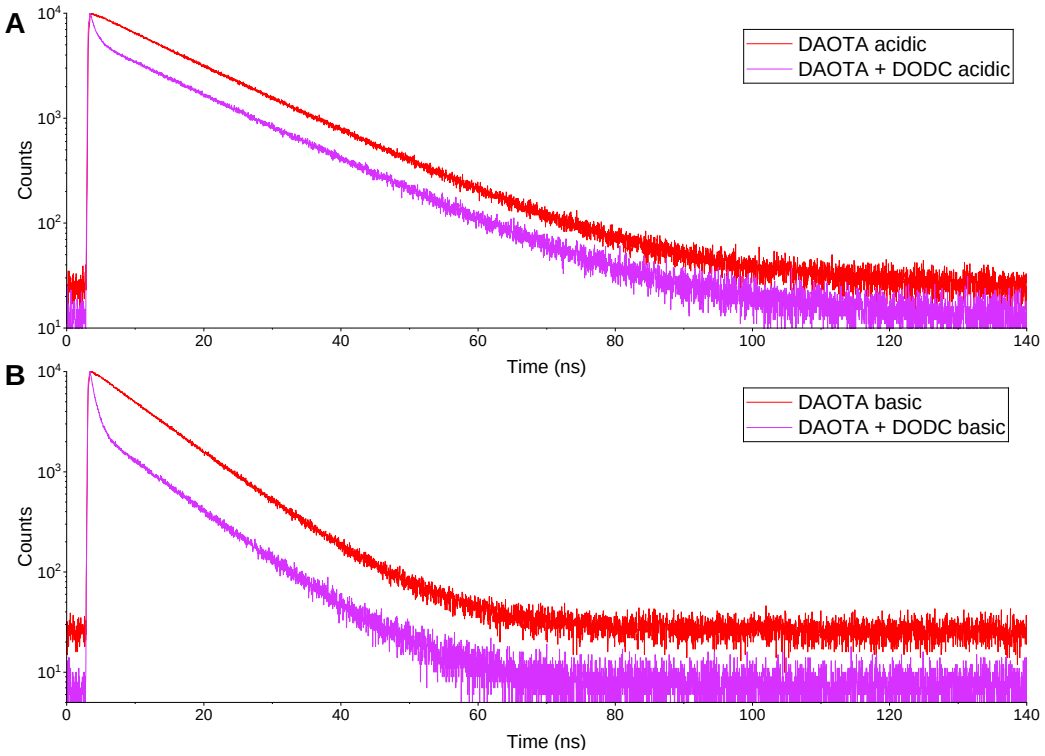

Figure S31. Fluorescence decays of phenol-DAOTA (red traces) and with addition of DODC (pink traces) in 100 mM phosphate buffer in A) acidic conditions and B) basic conditions.

The fluorescence lifetime of phenol-DAOTA in acidic and basic solution with the addition of DODC can be determined by reconvolution fitting 2 exponentials or by tail fitting (omitting data from 0-5 ns after prompt) effectively gating the DODC signal away. Both fitting methods for the decays with DODC, as the autofluorescent species, yielded the expected lifetime of phenol-DAOTA, as shown in Figure S31.

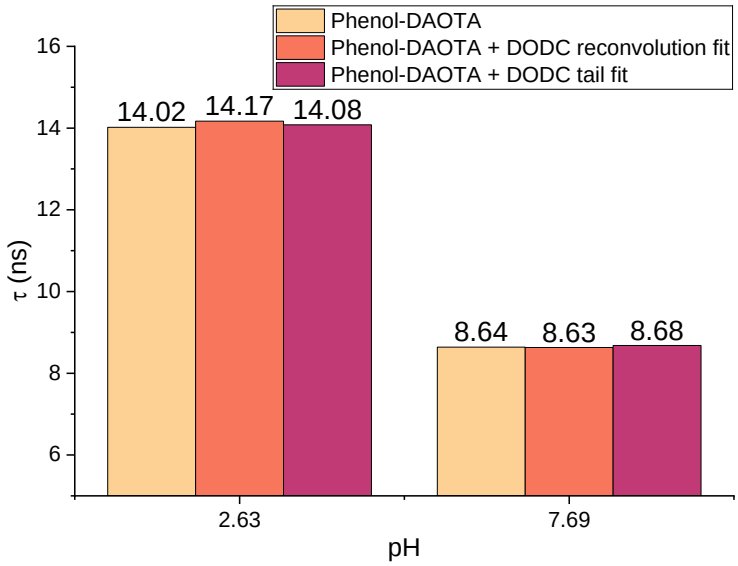

Figure S32. Fluorescence lifetimes of phenol-DAOTA in 100 mM phosphate buffer in acidic and basic conditions.

§12. Fluorescence lifetime measurements

Decays measured in acetate buffer (Figure S32) and representative lifetime fits (Figure S33-35).

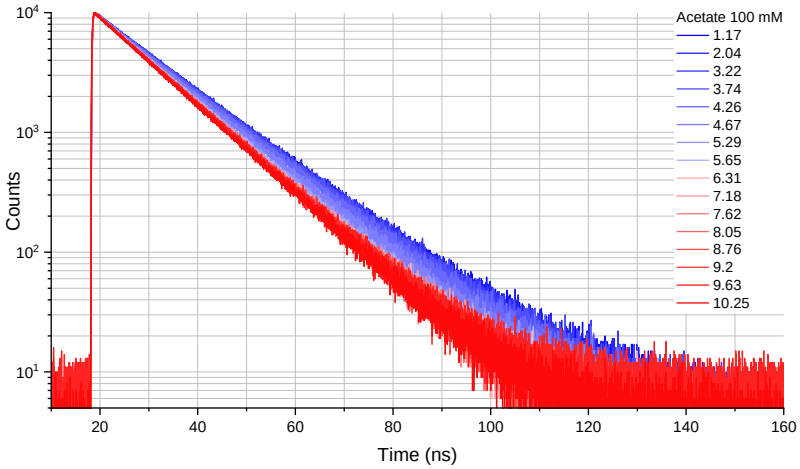

Figure S33. Fluorescence decays measured in acetate buffer 100 mM at pH ranging from 1.17 to 10.15.

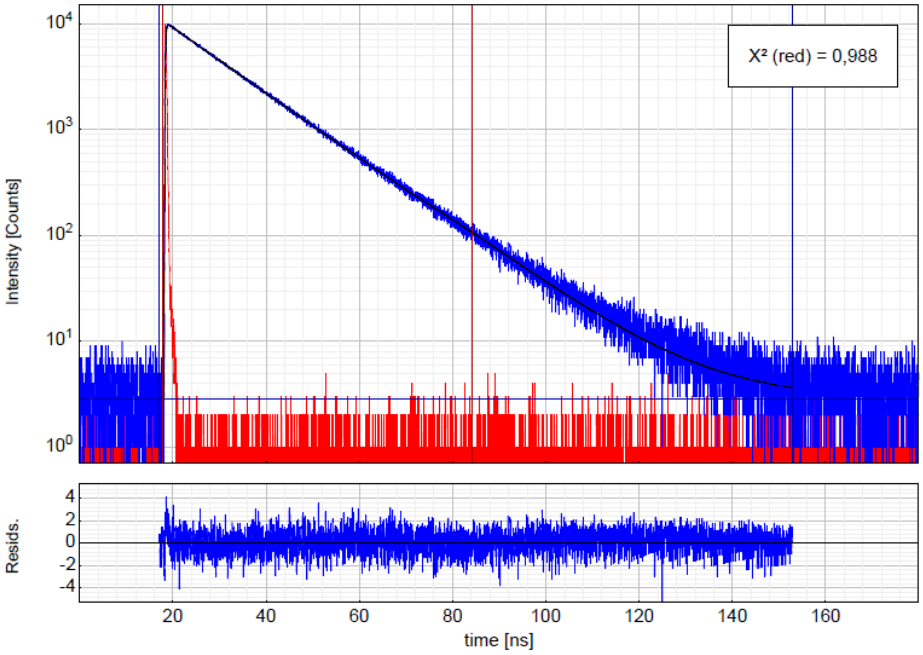

Figure S34. Fluorescence decay and fit measured in acetate buffer 100 mM at pH 1.17.

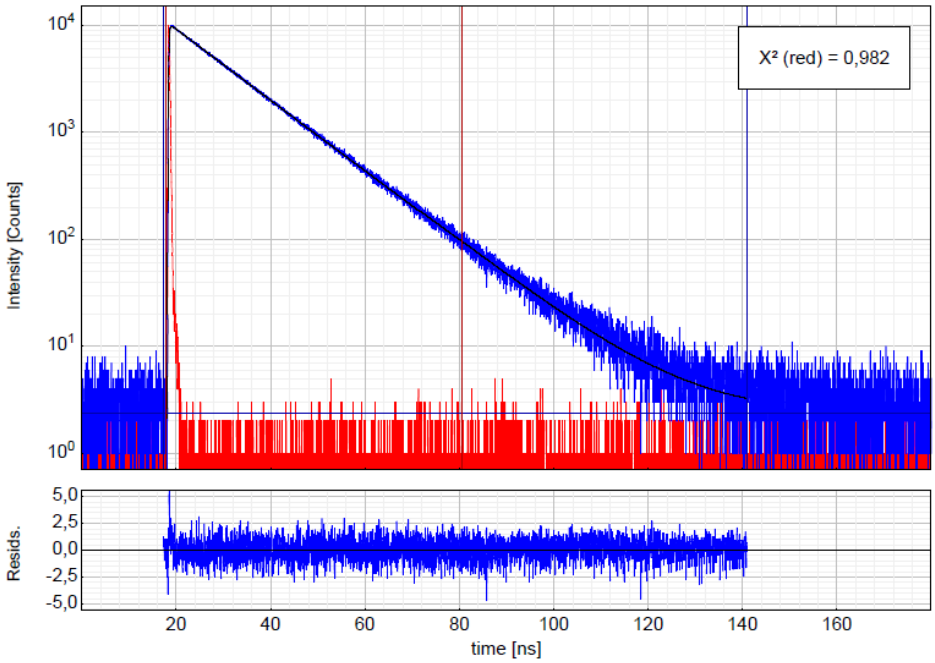

Figure S35. Fluorescence decay and fit measured in acetate buffer 100 mM at pH 4.67.

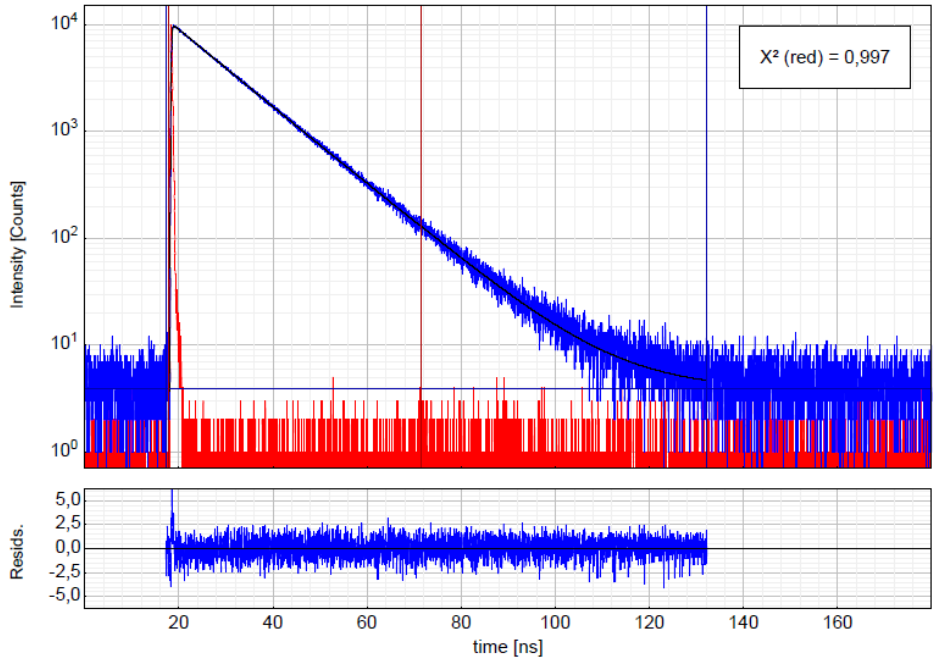

Figure S36. Fluorescence decay and fit measured in acetate buffer 100 mM at pH 9.20.

References

1. Rosenberg, M.; Junker, A. K. R.; Sorensen, T. J.; Laursen, B. W., Fluorescence pH Prob es Based on Photoinduced Electron Transfer Quenching of Long Fluorescence Lifetime Triangulenium Dyes. *Chemphotochem* **2019,** *3* (5), 233-242.
2. Lide, D. R.; Frederikse, H. P. R., *CRC handbook of chemistry and physics : a ready-reference book of chemical and physical data*. 75. ed. ed.; CRC Press: 1994.
3. Green, A. A., The Preparation of Acetate and Phosphate Buffer Solutions of Known PH and Ionic Strength. *Journal of the American Chemical Society* **1933,** *55* (6), 2331-2336.
4. Kumler, W. D.; Eiler, J. J., The Acid Strength of Mono and Diesters of Phosphoric Acid. The n-Alkyl Esters from Methyl to Butyl, the Esters of Biological Importance, and the Natural Guanidine Phosphoric Acids. *Journal of the American Chemical Society* **1943,** *65* (12), 2355-2361.
5. Bunton, C. A.; Chaimovich, H., The Hydrolysis of Glucose 6-Phosphate1,2. *Journal of the American Chemical Society* **1966,** *88* (17), 4082-4089.
6. Degani, C.; Halmann, M., Solvolysis of Phosphoric Acid Esters. Hydrolysis of Glucose 6-Phosphate. Kinetic and Tracer Studies. *Journal of the American Chemical Society* **1966,** *88* (17), 4075-4082.
7. Eigen, M., Proton Transfer, Acid-Base Catalysis, and Enzymatic Hydrolysis. Part I: ELEMENTARY PROCESSES. *Angewandte Chemie International Edition in English* **1964,** *3* (1), 1-19.
8. Bell, R. P., *The Proton in Chemistry*. 2 ed.; Chapman and Hall: London, 1973.
9. Lide, D. R.; Frederiksen, H. P. R., *CRC handbook of chemistry and physics : a ready reference book of chemical and physical data.* 75 ed.; CRC press: 1994.
10. Longsworth, L. G., Diffusion Measurements, at 25°, of Aqueous Solutions of Amino Acids, Peptides and Sugars. *J. Am. Chem. Soc.* **1953,** *75* (22), 5705-5709.
11. Jakobsen, R. K.; Laursen, B. W., New Principle for Simple Water Detection using Fluorescence Lifetime Triangulenium Probes. *ChemPhotoChem* **2024,** *8* (2), e202300215.